Multibody Syst Dyn (2010) 23: 361–386
DOI 10.1007/s11044-010-9194-y

Intrinsic deformable joints

Pierangelo Masarati · Marco Morandini

Received: 9 September 2009 / Accepted: 9 February 2010 / Published online: 4 March 2010

Abstract This paper addresses the problem of reducing the constitutive behavior of relatively complex mechanical systems to lumped deformable components that connect two nodes of a multibody system. It is common practice, both in finite element and multibody system dynamics analysis, to refer the constitutive properties of lumped components to one of the nodes they connect. It is shown that this practice, here termed "attached," could result in either underestimating or overestimating the couplings related to the finiteness of the relative rotation between the connected nodes. This work proposes an alternative formulation, here termed "intrinsic" that allows to correlate very well the behavior of general lumped deformable components with that resulting from the nonlinear finite element analysis of three-dimensional models of the components. Numerical examples, including the analysis of components that are widely used in the mechanical and aerospace industry, show how the proposed formulation can easily and accurately account for nonlinear geometrical effects, and thus deliver compact and accurate models suitable for the analysis of the global behavior of rather complex components.

Keywords Structures · Constitutive equations · Elasticity · Nonlinear dynamics

1 Introduction

In Finite Element Analysis (FEA), it is common practice to separate connectivity and constitutive properties when defining the contribution of structural elements to the equations that describe the problem. This feature, introduced from the beginning in the most popular FEA software, like MSC/NASTRAN and Abaqus, just to mention a few, typically had the purpose of simplifying model preparation by introducing a level of indirection in structural properties assignment to sets of elements.

P. Masarati (✉) · M. Morandini
Dipartimento di Ingegneria Aerospaziale, Politecnico di Milano, via La Masa 34, 20156 Milan, Italy
e-mail: pierangelo.masarati@polimi.it

M. Morandini
e-mail: marco.morandini@polimi.it

Another common practice in structural modeling consists in synthesizing complex structural components, whose main purpose consists in connecting larger model portions into lumped deformable components whenever their detailed analysis is either not strictly required, or beyond the scope of the analysis. This is especially true when the main focus is on the global dynamical behavior of complex mechanical systems, where detailed structural analysis is not required and would unnecessarily increase the computational time and cost.

At the very beginning, multibody dynamics addressed the analysis of rigid mechanisms undergoing arbitrary finite motion [1]. An outstanding review of the problems and solution approaches proposed in the early years is presented in [2], along with a discussion on future challenges. Whenever required, the flexibility of bodies was accounted for by means of lumped components.

Soon, the need to deal with more detailed models of rather complex structural components required the introduction of direct deformable system modeling capabilities in multibody analysis software. Many formulations have been proposed in the literature to bridge the gap between detailed FEA and multibody dynamics. Reviews are presented in [3, 4]. The research in this area was initially biased by the attempt to exploit linear FEA to model system flexibility, by separating the overall rigid-body motion of mechanism components from the local motion related to components' flexibility. This is often termed the *floating frame* approach [1, 5]. It is usually based on model reduction techniques to obtain a simple form of the strain energy, under the assumption of infinitesimal strains, thus resulting in the linear superimposition of simple deformation shapes, computed by means of linear FEA. This approach has been also extended to account for nonlinearities, both geometrical, like prestress (e.g. [6]), and plasticity (e.g. [7]). However, the need to drop the infinitesimal strain assumption in a consistent manner pushed toward the direct use of nonlinear FEA [5, 8], also in the form of absolute coordinates [9].

At the same time, considerable attention was given to the problem of synthesizing accurate constitutive properties for the modeling of joints whose behavior is time-dependent, like bushings, characterized by complex rheological behavior ([10, 11], to mention a few). It is worth stressing that the literature on this specific subject seldom addresses components with more than one dimension.

Much like multibody codes, a vast majority of FEA implementations supports the modeling of lumped structural elements. When linear analysis is considered, this procedure does not pose any specific issue. However, this might be no longer true when nonlinear analysis, encompassing finite displacements and rotations, must be considered. Recent structural analysis software implementations, either specifically intended for multibody system analysis, like MSC/ADAMS, or for nonlinear FEA with multibody capabilities, like Abaqus/Standard, allow arbitrarily large absolute displacements and rotations of the nodes and correctly describe their rigid-body motion. However, they occasionally require relative displacements and rotations to be limited, although not necessarily infinitesimal, when lumped deformable components modeling is concerned. For example, this occurs with MSC/ADAMS when using the `FIELD` element (a linear element based on a constant, orthotropic constitutive matrix [12]), to implement an orthotropic angular spring. Similarly, the `JOINTC` element implemented in Abaqus/Standard, describes the interaction between two nodes when the second node can "displace and rotate slightly with respect to the first node" [13], since its formulation is based on an approximate relative rotation measure (see Appendix A for details).

None of the lumped deformable component formulations and implementations available in commercial software appears to allow arbitrarily large relative displacements and, significantly, rotations. In most cases, moreover, the ordering of the connected nodes matters,

since the behavior of the lumped deformable component is biased with respect to one of the nodes. This problem seems to be quite intuitive, and should be well known to experienced analysts. However, the fact that no specific mention of it can be found in the literature, to the authors' knowledge, and little effort has been put into eliminating it from the formulations commercially available software is based on seems to indicate that it has always been overlooked, although its implications might lead to unexpected results. The problem was recently anticipated and discussed in [14], in the context of rubber component modeling within applications in the automotive field.

This work aims at formulating a lumped deformable component, based on a consistent definition of the nonlinear strain, independent from the constitutive behavior, giving up the detail provided by direct nonlinear FEA but with much less computational cost. The work also aims at pointing out the effects of connectivity modeling on the behavior of lumped components, to allow to decouple them as much as possible from the constitutive behavior. This is accomplished by:

1. Introducing a rigorous definition of the linear and angular strains as the actual relative displacement and rotation between the nodes connected by the deformable joint; and
2. Introducing the possibility to arbitrarily refer the constitutive properties to a reference frame that depends on the relative orientation.

The objective is to either:

(a) Produce a formulation that does not depend on the ordering of the connectivity, for ease of use and robustness with respect to inexperienced user's errors or alternatively.
(b) Allow fine-grained tuning of the joint behavior in order to match experimentally or numerically determined load-strain curves.

A definition of *deformable joint* is given in Sect. 2, while Sect. 3 presents the deformable joint formulation termed *intrinsic*, which in noteworthy cases specializes in the *attached* and *invariant* forms. Section 4 presents and discusses numerical applications that highlight the issues the intrinsic formulation is intended to overcome. Relevant details are presented in Appendices.

2 Deformable joint formulation

The term *deformable joint* is intended to indicate a relationship between the relative configuration of two nodes (the relative position and orientation) and the corresponding forces and moments each node exchanges with the other.

Consider a deformable joint connecting two nodes, respectively indicated with subscripts a and b. When strained by a relative rotation vector $\boldsymbol{\theta}$ and a change in relative position $\mathbf{d}$ (respectively defined in Sects. 2.2 and 2.3), the joint can apply to each node the respective forces and moments indicated in (1):

$$\mathbf{f}_i = \mathbf{f}_i(\boldsymbol{\theta}, \mathbf{d}), \tag{1a}$$

$$\mathbf{m}_i = \mathbf{m}_i(\boldsymbol{\theta}, \mathbf{d}), \tag{1b}$$

where $i = a, b$ refers to each node. The forces and moments of (1) are conjugated to the nodes' virtual displacements and rotations, as resulting from the virtual work related to the structural component,

$$\delta\mathcal{L} = \sum_{i=a,b} (\delta\mathbf{x}_i \cdot \mathbf{f}_i + \boldsymbol{\theta}_{i\delta} \cdot \mathbf{m}_i). \tag{2}$$

The rotation perturbation vector $\boldsymbol{\theta}_\delta$ results from perturbing a rotation matrix[1] $\mathbf{R}$,

$$\delta\mathbf{R}\mathbf{R}^T = \boldsymbol{\theta}_\delta \times . \tag{3}$$

In some configurations, a deformable joint may not contribute to the dynamics equations with all combinations of forces and moments, or it may only depend on the relative orientation (angular strain) or position (linear strain), resulting in a lumped deformable component that is a specialization of the most general one.

2.1 Connectivity and constitutive properties

When implementation issues are considered, significant advantages can be obtained by separating the connectivity from the constitutive properties of a deformable joint.

The term *connectivity* is used here in the sense of determining how the measurement of the straining of the joint is computed from the relative configuration of the connected nodes. In the case of an angular joint, it determines how a suitable measure of the change in relative orientation is extracted from the orientations of the two nodes connected by the joint, whereas in the case of a linear joint it determines how a suitable measure of the change in relative position is extracted from the positions and orientations of the nodes connected by the joint.

The *constitutive properties*, in turn, represent the relationship between the selected strain measure and the corresponding forces and moments exchanged between the nodes connected by the joint.

By separating these two aspects of the formulation of deformable joints, a software implementation of a multibody formalism can arbitrarily couple different connectivities and different constitutive relationships with minimal code duplication and development effort. This consideration is *per se* by no means novel; in fact, it is deeply rooted in most of the FEA formulations.

What this work intends to highlight is the fact that the separation between connectivity and constitutive properties may not be trivial when finite relative rotations take place. Based on the assumption that the actual behavior of a deformable component cannot be altered by the choice of the reference frame used to express its constitutive properties, it is observed that the choice of that reference frame may affect the way in which the joint's constitutive properties have to be formulated, and actually allow to decouple constitutive from connectivity aspects of that behavior.

Relevant properties of angular and linear joints connecting two nodes are discussed in the following. Unless otherwise stated, no bias toward a specific node is assumed.

2.2 Angular deformable joint

Within this work, the term *angular* joint refers to a deformable component whose strain measure is *a change in the relative orientation* between the nodes it connects.

This type of deformable component introduces a moment $\mathbf{m}$ that depends on the relative rotation between two nodes. Without significant loss in generality,[2] the relative rotation is

[1] A rotation matrix is orthonormal, i.e., $\mathbf{R}\mathbf{R}^T = \mathbf{R}^T\mathbf{R} = \mathbf{I}$. Its perturbation yields $\delta\mathbf{R}\mathbf{R}^T = -\mathbf{R}\delta\mathbf{R}^T = -(\delta\mathbf{R}\mathbf{R}^T)^T$, which implies that matrix $\delta\mathbf{R}\mathbf{R}^T$ is skew-symmetric; thus, it can be represented as $\boldsymbol{\theta}_\delta \times .$

[2] The main limitation introduced by the definition given in (4) is in the magnitude of $\boldsymbol{\theta}$, $\|\boldsymbol{\theta}\| < \pi$. This limitation can be removed, if required, by considering an incremental formulation, not pursued in the present work essentially for clarity.

described by the rotation matrix

$$\mathbf{R}_{\text{rel}} = \mathbf{R}_a^T \mathbf{R}_b, \tag{4}$$

where $\mathbf{R}_i$, $i = a, b$, are the orientation matrices of nodes a and b. The relative orientation, in turn, can be described by the vector[3] $\boldsymbol{\theta}$, defined as

$$\boldsymbol{\theta} = \text{ax}\big(\exp^{-1}(\mathbf{R}_{\text{rel}})\big). \tag{5}$$

The operator $\exp^{-1}(\cdot)$ in (5) is the inverse operator[4] of the exponential map operator $\exp(\cdot)$, while operator $\text{ax}((\cdot) \times)$ is the inverse of the cross-product operator, $(\cdot)\times$. A numerically stable algorithm for (5) is presented in Appendix 2.4 of [18]. The direction of vector $\boldsymbol{\theta}$ describes the axis about which the rotation indicated by $\mathbf{R}_{\text{rel}}$ occurs, while its modulus describes the magnitude of the rotation.

This strain measure is intrinsic, because it is based only on the relative orientation of the two bodies, regardless of its representation. It is also invariant, in the sense that vector $\boldsymbol{\theta}$, defined by (5) in the reference frame of node a, does not change when it is projected in that of node b: (5) implies that

$$\begin{aligned} \boldsymbol{\theta} &= \mathbf{R}_{\text{rel}} \boldsymbol{\theta} \\ &= \mathbf{R}_{\text{rel}}^T \boldsymbol{\theta}, \end{aligned} \tag{6}$$

which can be restated by noticing that $\boldsymbol{\theta}$ is parallel to the eigenvector associated with the unit eigenvalue of matrix $\mathbf{R}_{\text{rel}}$.

2.3 Linear deformable joint

Within this work the term *linear* joint refers to a deformable component whose strain measure is a *change in the relative position* between the nodes it connects. What makes this connectivity model more complicated than the angular one is that both the connectivity and the constitutive properties may also depend on the relative orientation between the connected nodes.

This type of deformable component introduces a force $\mathbf{f}$ that depends on a change in the relative position between two nodes. The point where this force is applied depends on the way its connectivity is formulated, and thus may result in a moment with respect to the points $\mathbf{x}_a$ and $\mathbf{x}_b$ used as references for the position of the nodes. The strain measure is described by the vector that represents the distance between two reference points $\mathbf{p}_a$ and $\mathbf{p}_b$

$$\mathbf{d} = \mathbf{p}_b - \mathbf{p}_a, \tag{7}$$

which vanishes when the joint is unloaded. These points may be offset from the reference positions of the nodes by the vectors $\mathbf{o}_a$ and $\mathbf{o}_b$,

$$\mathbf{p}_i = \mathbf{x}_i + \mathbf{o}_i, \tag{8}$$

[3] This vector is often termed "rotation vector," a name widely used in the literature to indicate the Euler vector; see, for instance [15–17].

[4] In the literature, the operator $\exp^{-1}(\cdot)$ is also indicated as $\log(\cdot)$, e.g. [18, 19].

with $i = a, b$ as before. The offsets $\mathbf{o}_i$ are assumed to be constant in the reference frames of the respective nodes. As a consequence, the distance of (7) is

$$\mathbf{d} = \mathbf{x}_b + \mathbf{o}_b - \mathbf{x}_a - \mathbf{o}_a. \tag{9}$$

This strain measure is also intrinsic, because it is based only on the relative position of the two bodies, regardless of its representation.

Although by definition this component only associates the strain measure to the relative position of the bodies, the relative orientation comes into play because it can affect not only the way in which the strain measure is related to the constitutive properties in the case of anisotropy, but also the virtual point the straining is supposed to occur at, when $\mathbf{o}_i \neq \mathbf{0}$.

2.4 Linear/angular deformable joint

Within this work, the term *linear/angular* joint refers to a deformable component whose strain measure is a *change in both the relative position and orientation* between the nodes it connects. What distinguishes the linear/angular joint from a mere combination of a linear and an angular joint is the fact that its constitutive law may arbitrarily depend on both strain measures. However, the formulation of this latter component is not discussed in detail *per se*, since apart from additional implementation issues it does not add significant insight into the subject of this work. On the contrary, its application lends itself to interesting and detailed considerations that will be illustrated in Sect. 4.2.

In principle, this joint is analogous to a two-node beam element. Its constitutive properties result from the integration of the strain energy associated to the relative motion of the two nodes. However, there is no slenderness nor smoothness requirement in the direction loosely identified as the beam axis. A formal proof of this statement, in case of a beam-like structure, is beyond the scope of this work.

3 The "intrinsic" formulation

A common choice of the reference frame for the formulation of the constitutive properties of a deformable joint consists in a frame that is rigidly attached to one of the parts connected by the joint. The joint itself can be experimentally characterized by measuring the forces and moments related to imposed changes in the relative position and orientation of the connected parts, and by expressing those measures in that reference frame. This is particularly practical when the loads are measured by balances or gages connected to one of the parts. Of course, the use of those constitutive properties needs to be consistent with the way they have been defined or measured. Hence, the constitutive law in the model needs to be referred to a reference frame that is rigidly attached to the same part that was used for the characterization.

However, (6) suggests that any relative orientation described by a vector parallel to $\boldsymbol{\theta}$, and whose magnitude is comprised between 0 and that of $\boldsymbol{\theta}$, represents an intermediate orientation resulting from the weighting of the orientations of the two nodes. This approach is common practice, for example, in many applications that need to interpolate orientations for visualization purposes [20]. It has been used for the formulation of beam finite elements [21, 22]. It has also been generalized to the interpolation over more than two orientations as required, for example, in shell elements, and in solid elements when used in conjunction with polar continua [19].

Consider a vector

$$\tilde{\boldsymbol{\theta}}(\xi) = \xi\boldsymbol{\theta}, \tag{10}$$

with $\xi \in \mathbb{R}$, yielding an orientation matrix

$$\begin{aligned}\tilde{\mathbf{R}}\big(\tilde{\boldsymbol{\theta}}(\xi)\big) &= \exp\big(\tilde{\boldsymbol{\theta}}(\xi)\times\big)\\ &= \exp\big((\xi\boldsymbol{\theta})\times\big).\end{aligned} \tag{11}$$

When $\xi \in [0, 1]$, this matrix allows to define an intermediate orientation between those of the two nodes; this is not strictly required, as illustrated in the numerical examples. This matrix also possesses the property of (6), since it is constructed from a vector parallel to $\boldsymbol{\theta}$.

The relative orientation between the connected nodes can be expressed as

$$\mathbf{R}_{\text{rel}} = \tilde{\mathbf{R}}\big(\tilde{\boldsymbol{\theta}}(\xi)\big)\tilde{\mathbf{R}}\big(\tilde{\boldsymbol{\theta}}(1-\xi)\big). \tag{12}$$

Matrix $\tilde{\mathbf{R}}(\tilde{\boldsymbol{\theta}}(\xi))$ of (11) is used to project the constitutive properties in a reference frame resulting from the consistent weighting of the orientations of the connected nodes. The resulting formulation has been termed "intrinsic" since it depends on an intrinsic measure of the linear and angular strains, despite the degree of arbitrarity introduced by the choice of ξ. This section and the numerical examples of Sect. 4 show how this arbitrarity can be exploited.

When $\xi = 0$, the constitutive properties are referred to the first node connected by the joint. This case has been termed "attached." The case of $\xi = 1$ results from reversing the order of the connected nodes, thus it is not explicitly dealt with.

A special case occurs when $\xi = 1/2$; the resulting intrinsic element is also termed "invariant," since its behavior does not depend on the ordering of the element's connectivity. In the following, when the argument is omitted the entities under a tilde $\tilde{(\cdot)}$ are evaluated for $\xi = 1/2$, namely $\tilde{\boldsymbol{\theta}} = \boldsymbol{\theta}/2$ and thus $\tilde{\mathbf{R}} = \exp(\tilde{\boldsymbol{\theta}}\times)$. In this case, the relative orientation matrix of (12) can be represented as

$$\mathbf{R}_{\text{rel}} = \tilde{\mathbf{R}}\tilde{\mathbf{R}} = \tilde{\mathbf{R}}^2. \tag{13}$$

When the orientation $\tilde{\mathbf{R}}$ is used, the constitutive properties are intrinsically expressed in the reference frame defined by $\tilde{\boldsymbol{\theta}}$, which is halfway in between the relative orientation of the nodes.

Interestingly enough, a similar approach has been proposed for conservative time integration of rotations [23], where the selection of the orientation halfway in between the initial and the final orientations of a body during a time step is used to construct a vectorial representation of the finite rotation over the time step, essentially based on Cayley's transform and its properties.

3.1 Angular deformable joint

The moment $\mathbf{m}$ exchanged by the two bodies is indicated as $\overline{\mathbf{m}}(\boldsymbol{\theta})$. The same moment, in the reference frame of nodes a and b, is

$$\mathbf{m}(\boldsymbol{\theta})|_a = \tilde{\mathbf{R}}\big(\tilde{\boldsymbol{\theta}}(\xi)\big)\overline{\mathbf{m}}(\boldsymbol{\theta}), \tag{14a}$$

$$\mathbf{m}(\boldsymbol{\theta})|_b = \tilde{\mathbf{R}}\big(\tilde{\boldsymbol{\theta}}(1-\xi)\big)^T\overline{\mathbf{m}}(\boldsymbol{\theta}). \tag{14b}$$

It is clear from (14) that the definition of the moment with respect to both nodes can be the same only when the moment $\overline{\mathbf{m}}(\boldsymbol{\theta})$ is structurally parallel to $\boldsymbol{\theta}$. This can only occur when the constitutive law is isotropic, and thus

$$\overline{\mathbf{m}}(\boldsymbol{\theta}) = m(\boldsymbol{\theta}) \frac{\boldsymbol{\theta}}{\|\boldsymbol{\theta}\|}. \tag{15}$$

When $\xi = 0$, (14) result in

$$\mathbf{m}(\boldsymbol{\theta})|_a = \overline{\mathbf{m}}(\boldsymbol{\theta}), \tag{16a}$$

$$\mathbf{m}(\boldsymbol{\theta})|_b = \mathbf{R}_{\text{rel}}^T \overline{\mathbf{m}}(\boldsymbol{\theta}). \tag{16b}$$

These equations clearly show how the moment applied to the connected nodes is biased toward the orientation of the first node.

When $\xi = 1/2$, (14) result in

$$\mathbf{m}(\boldsymbol{\theta})|_a = \tilde{\mathbf{R}}\overline{\mathbf{m}}(\boldsymbol{\theta}), \tag{17a}$$

$$\mathbf{m}(\boldsymbol{\theta})|_b = \tilde{\mathbf{R}}^T \overline{\mathbf{m}}(\boldsymbol{\theta}), \tag{17b}$$

which clearly show how the re-orientation of the constitutive property $\overline{\mathbf{m}}(\boldsymbol{\theta})$ from the intermediate relative orientation to that of either node is characterized by the same relative rotation $\tilde{\mathbf{R}}$, in opposite directions.

The contribution of the intrinsic angular strain joint to the equations of the problem results from the virtual work contribution

$$\delta\mathcal{L} = \boldsymbol{\theta}_\delta \cdot \tilde{\mathbf{R}}\big(\tilde{\boldsymbol{\theta}}(\xi)\big)\overline{\mathbf{m}}(\boldsymbol{\theta}). \tag{18}$$

The contributions to the moment equilibrium equations of nodes a and b are

$$\mathbf{m}_a = -\hat{\mathbf{R}}\big(\tilde{\boldsymbol{\theta}}(\xi)\big)\overline{\mathbf{m}}, \tag{19a}$$

$$\mathbf{m}_b = \hat{\mathbf{R}}\big(\tilde{\boldsymbol{\theta}}(\xi)\big)\overline{\mathbf{m}}, \tag{19b}$$

where

$$\hat{\mathbf{R}}\big(\tilde{\boldsymbol{\theta}}(\xi)\big) = \mathbf{R}_a \tilde{\mathbf{R}}\big(\tilde{\boldsymbol{\theta}}(\xi)\big) \tag{20a}$$

$$= \mathbf{R}_b \tilde{\mathbf{R}}\big(\tilde{\boldsymbol{\theta}}(1-\xi)\big)^T; \tag{20b}$$

when $\xi = 1/2$, $\hat{\mathbf{R}} = \hat{\mathbf{R}}(\tilde{\boldsymbol{\theta}})$.

3.2 Linear deformable joint

The force $\overline{\mathbf{f}}$ exchanged by the two bodies, indicated as $\overline{\mathbf{f}}(\overline{\mathbf{d}})$, is expressed in the weighted relative orientation of (20a). The relative position $\overline{\mathbf{d}}$, which is expressed in the same reference frame, is

$$\overline{\mathbf{d}}(\xi) = \hat{\mathbf{R}}\big(\tilde{\boldsymbol{\theta}}(\xi)\big)^T \mathbf{d}. \tag{21}$$

The force, in the reference frames of the nodes, is

$$\mathbf{f}\big(\overline{\mathbf{d}}(\xi)\big)\Big|_a = \tilde{\mathbf{R}}\big(\tilde{\boldsymbol{\theta}}(\xi)\big)\overline{\mathbf{f}}\big(\overline{\mathbf{d}}(\xi)\big), \tag{22a}$$

$$\mathbf{f}\big(\overline{\mathbf{d}}(\xi)\big)\Big|_b = \tilde{\mathbf{R}}\big(\tilde{\boldsymbol{\theta}}(1-\xi)\big)^T \bar{\mathbf{f}}\big(\overline{\mathbf{d}}(\xi)\big); \tag{22b}$$

when the relative position is written in the same reference of the forces,

$$\mathbf{f}(\mathbf{d}|_a)|_a = \tilde{\mathbf{R}}\big(\tilde{\boldsymbol{\theta}}(\xi)\big)\bar{\mathbf{f}}\big(\tilde{\mathbf{R}}\big(\tilde{\boldsymbol{\theta}}(\xi)\big)^T\,\mathbf{d}|_a\big), \tag{23a}$$

$$\mathbf{f}(\mathbf{d}|_b)|_b = \tilde{\mathbf{R}}\big(\tilde{\boldsymbol{\theta}}(1-\xi)\big)^T \bar{\mathbf{f}}\big(\tilde{\mathbf{R}}\big(\tilde{\boldsymbol{\theta}}(1-\xi)\big)\,\mathbf{d}|_b\big). \tag{23b}$$

Since no particular relationship exists between the relative displacement $\mathbf{d}$ and the relative orientation $\boldsymbol{\theta}$ that characterizes $\mathbf{R}_{\text{rel}}$, the two representations of the force $\mathbf{f}$ always differ.

The contribution of the intrinsic linear strain joint to the equations of the problem results from the virtual work contribution

$$\delta\mathcal{L} = \delta\overline{\mathbf{d}}(\xi)\cdot\bar{\mathbf{f}}\big(\overline{\mathbf{d}}(\xi)\big). \tag{24}$$

Vector $\hat{\boldsymbol{\theta}}_\delta(\xi)$, resulting from the perturbation of matrix $\hat{\mathbf{R}}(\tilde{\boldsymbol{\theta}}(\xi))$, is

$$\hat{\boldsymbol{\theta}}_\delta(\xi) = \hat{\mathbf{I}}(\xi)\boldsymbol{\theta}_{b\delta} + \hat{\mathbf{I}}(1-\xi)^T\boldsymbol{\theta}_{a\delta}, \tag{25}$$

with

$$\hat{\mathbf{I}}(\xi) = \xi\hat{\mathbf{R}}\big(\tilde{\boldsymbol{\theta}}(\xi)\big)\boldsymbol{\Gamma}\big(\tilde{\boldsymbol{\theta}}(\xi)\big)\boldsymbol{\Gamma}(\boldsymbol{\theta})^{-1}\hat{\mathbf{R}}\big(\tilde{\boldsymbol{\theta}}(\xi)\big)^T. \tag{26}$$

Tensor $\boldsymbol{\Gamma}$ is defined by the relationship (see for example [24])

$$\boldsymbol{\theta}_\delta = \boldsymbol{\Gamma}(\boldsymbol{\theta})\delta\boldsymbol{\theta}. \tag{27}$$

As proved in Appendix B,

$$\hat{\mathbf{I}}(\xi) + \hat{\mathbf{I}}(1-\xi)^T = \mathbf{I}, \tag{28}$$

thus the perturbation of the linear strain measure is

$$\begin{aligned}\delta\overline{\mathbf{d}}(\xi) &= \hat{\mathbf{R}}\big(\tilde{\boldsymbol{\theta}}(\xi)\big)^T\big(\delta\mathbf{d} - \mathbf{d}\times\hat{\boldsymbol{\theta}}_\delta(\xi)\big)\\ &= \hat{\mathbf{R}}\big(\tilde{\boldsymbol{\theta}}(\xi)\big)^T\Big(\delta\mathbf{x}_b - \big(\mathbf{o}_b\times - \hat{\mathbf{I}}(\xi)\big)\boldsymbol{\theta}_{b\delta} - \delta\mathbf{x}_a + \big(\mathbf{o}_a\times + \hat{\mathbf{I}}(1-\xi)^T\big)\boldsymbol{\theta}_{a\delta}\Big).\end{aligned} \tag{29}$$

As a consequence, the contribution of this component to the force and moment equilibrium equations of nodes a and b, in the global reference frame, is

$$\mathbf{f}_a = -\hat{\mathbf{R}}\big(\tilde{\boldsymbol{\theta}}(\xi)\big)\bar{\mathbf{f}}, \tag{30a}$$

$$\mathbf{m}_a = -\big(\mathbf{o}_a\times + \hat{\mathbf{I}}(1-\xi)\mathbf{d}\times\big)\hat{\mathbf{R}}\big(\tilde{\boldsymbol{\theta}}(\xi)\big)\bar{\mathbf{f}}, \tag{30b}$$

$$\mathbf{f}_b = \hat{\mathbf{R}}\big(\tilde{\boldsymbol{\theta}}(\xi)\big)\bar{\mathbf{f}}, \tag{30c}$$

$$\mathbf{m}_b = \big(\mathbf{o}_b\times - \hat{\mathbf{I}}(\xi)^T\mathbf{d}\times\big)\hat{\mathbf{R}}\big(\tilde{\boldsymbol{\theta}}(\xi)\big)\bar{\mathbf{f}}. \tag{30d}$$

When $\xi = 0$, matrix $\hat{\mathbf{I}}(\xi)$ vanishes and $\hat{\mathbf{I}}(1-\xi) = \mathbf{I}$, so (30) become

$$\mathbf{f}_a = -\mathbf{R}_a\bar{\mathbf{f}}, \tag{31a}$$

$$\mathbf{m}_a = -(\mathbf{o}_a + \mathbf{d})\times\mathbf{R}_a\bar{\mathbf{f}}, \tag{31b}$$

$$\mathbf{f}_b = \mathbf{R}_a \bar{\mathbf{f}}, \tag{31c}$$

$$\mathbf{m}_b = \mathbf{o}_b \times \mathbf{R}_a \bar{\mathbf{f}}. \tag{31d}$$

When $\xi = 1/2$, matrix $\hat{\mathbf{I}}(\xi)$ can be written as

$$\hat{\mathbf{I}} = \hat{\mathbf{R}}(\mathbf{I} + \tilde{\mathbf{R}})^{-1} \hat{\mathbf{R}}^T, \tag{32}$$

so (30) become

$$\mathbf{f}_a = -\hat{\mathbf{R}} \bar{\mathbf{f}}, \tag{33a}$$

$$\mathbf{m}_a = -(\mathbf{o}_a \times + \hat{\mathbf{I}} \mathbf{d} \times) \hat{\mathbf{R}} \bar{\mathbf{f}}, \tag{33b}$$

$$\mathbf{f}_b = \hat{\mathbf{R}} \bar{\mathbf{f}}, \tag{33c}$$

$$\mathbf{m}_b = \left(\mathbf{o}_b \times - \hat{\mathbf{I}}^T \mathbf{d} \times\right) \hat{\mathbf{R}} \bar{\mathbf{f}}. \tag{33d}$$

Matrix $\hat{\mathbf{I}}$ possesses interesting invariance properties, detailed in Appendix C.

An interesting graphical interpretation of the linear strain in the proposed formulation is given in Fig. 1. Figure 1(i) shows that when the joint strains, points a and b are separated by the distance $\mathbf{d}$, the linear strain defined in (9). Figures 1(ii–iii) illustrate the cases of constitutive properties respectively attached, in terms of orientation, to the reference frames of nodes a and b. The unit vectors $\mathbf{e}_1$ and $\mathbf{e}_2$ represent the reference frame the constitutive properties

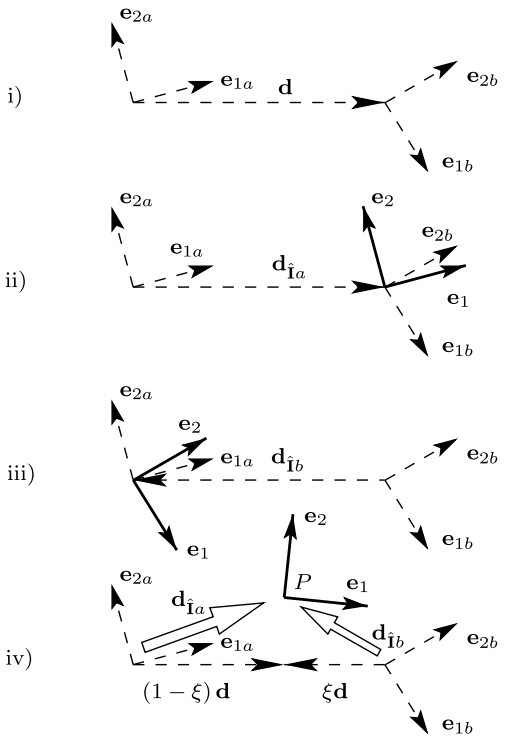

Fig. 1 Sketch of the linear/angular deformable joint: (**i**) node a and b orientation, linear strain $\mathbf{d}$; (**ii**) attached to node a ($\mathbf{d}_{\hat{\mathbf{I}}a} = \mathbf{d}\times$, $\mathbf{d}_{\hat{\mathbf{I}}b} = \mathbf{0}$); (**iii**) attached to node b ($\mathbf{d}_{\hat{\mathbf{I}}a} = \mathbf{0}$, $\mathbf{d}_{\hat{\mathbf{I}}b} = \mathbf{d}\times$); (**iv**) generic intrinsic case

are expressed in, respectively parallel to that of node a, Fig. 9(ii), and b, Fig. 9(iii). According to (31b) and (31d), the force is applied in the opposite node. The generic intrinsic case, illustrated in Fig. 1(iv), corresponds to evaluating the constitutive properties with reference to a weighted orientation that depends on the fraction ξ of the relative orientation between the nodes. The resulting moment cannot be simply expressed by defining a virtual point P where the force is applied, since tensors

$$\mathbf{d}_{\hat{\mathbf{i}}a} = \hat{\mathbf{I}}(1-\xi)\mathbf{d}\times, \tag{34a}$$

$$\mathbf{d}_{\hat{\mathbf{i}}b} = \hat{\mathbf{I}}(\xi)^T\mathbf{d}\times, \tag{34b}$$

that premultiply the force in (30b) and (30d) are not skew-symmetric. As a consequence, the generalized internal moments conjugated to the virtual rotation of the nodes cannot be interpreted only in terms of the cross-product of physical arms by the internal force. For this reason, point P in Fig. 1(iv) has been placed outside segment $\mathbf{d}$ for pictorial representation purposes, but $\mathbf{d}_{\hat{\mathbf{i}}a}$ and $\mathbf{d}_{\hat{\mathbf{i}}b}$ have not been represented as regular arrows.

3.3 Linear/angular deformable joint

As anticipated in Sect. 2.4, the linear/angular joint basically consists in the union of a linear and an angular joint, where both the force and the moment simultaneously depend on the linear and angular strain. As a consequence, its formulation does not differ from those of the components presented so far.

4 Numerical results

This section presents selected numerical results that show how the proposed formulation addresses the issues related to connectivity ordering and decoupling between connectivity and constitutive properties. The formulation has been implemented in the free multibody analysis software MBDyn [25] since version 1.3.1, released in August 2007.

4.1 Simple angular strain joint

In the following, a simple problem is considered. A couple is applied to a node grounded by a deformable hinge, thus $\mathbf{R}_a = \mathbf{I}$. The node orientation with respect to the ground is represented by matrix $\mathbf{R}_b$. In all cases, a constitutive law that is linear in the material frame, namely

$$\overline{\mathbf{m}} = \mathbb{K}\boldsymbol{\theta}, \tag{35}$$

is considered, where $\mathbb{K}$ is a constant, symmetric, positive definite matrix, and

$$\boldsymbol{\theta} = \mathrm{ax}\left(\exp^{-1}\left(\mathbf{R}_b^T\right)\right) \tag{36}$$

is the vector that describes the rotation of the node with respect to the ground. This choice is only used for simplicity and clarity of exposition; in fact, it is intended to highlight how the proposed formulation allows to capture geometrical nonlinear effects related to finite rotations that other approaches would overlook.

The constitutive properties are generically expressed in a reference frame that is rotated from the ground node by an arbitrary fraction ξ of the relative rotation $\boldsymbol{\theta}$, as indicated

in (10), resulting in the orientation matrix $\tilde{\mathbf{R}}(\tilde{\boldsymbol{\theta}}(\xi))$. The moment, in the reference frame of the ground, is

$$\mathbf{m} = \tilde{\mathbf{R}}\big(\tilde{\boldsymbol{\theta}}(\xi)\big)\overline{\mathbf{m}}. \tag{37}$$

Three different configurations are considered:

– "ground": the constitutive law is attached to the ground ($\xi = 0$); the moment that the joint transmits to the ground, in the reference frame of the ground itself, is

$$\mathbf{m} = \mathbb{K}\boldsymbol{\theta}; \tag{38}$$

the orientation of the constitutive law does not change when the joint strains.
– "node": the constitutive law is attached to the node ($\xi = 1$); the moment that the joint transmits to the ground, in the reference frame of the ground itself, is

$$\mathbf{m} = \mathbf{R}_b\mathbb{K}\boldsymbol{\theta}; \tag{39}$$

the orientation of the constitutive law changes when the joint strains.
– "invariant": the constitutive law is referred to an orientation that is halfway in between that of the node and that of the ground ($\xi = 1/2$). The moment that the joint transmits to the ground, in the reference frame of the ground itself, is

$$\mathbf{m} = \tilde{\mathbf{R}}\mathbb{K}\boldsymbol{\theta}; \tag{40}$$

also in this case the orientation of the constitutive law changes when the joint strains.

4.1.1 Angular strain joint invariance verification

This section illustrates the use of deformable joints in well-known structural dynamics software with respect to their connectivity bias when anisotropic constitutive properties are considered.

As a reference, a highly orthotropic linear constitutive matrix,

$$\mathbb{K} = \begin{bmatrix} k_1'' & 0 & 0 \\ 0 & k_2'' & 0 \\ 0 & 0 & k_3'' \end{bmatrix}, \tag{41}$$

is considered, with $k_1'' = 1.0$, $k_2'' = 10.0$, and $k_3'' = 100.0$ Nm/radian. This matrix is used to model an angular joint with MBDyn's `deformable hinge` element, with Abaqus/Standard's `JOINTC` element, and with MSC/ADAMS' `FIELD` element for comparison purposes. Results are reported in Table 1, and discussed in the following.

For the case of a joint attached to the ground, when a unit moment slightly skewed by an angle $\alpha = 0.01$ radian from the principal direction 1 is applied, namely

$$\mathbf{m} = \begin{Bmatrix} 0 \\ \sin\alpha \\ \cos\alpha \end{Bmatrix}, \tag{42}$$

an analytical solution is readily available. No attached analytical solution could be found for a joint attached to the floating node when a unit moment about global axis 3 is applied. The numerical solution of (39) with the moment of (42) is thus reported as reference. Similarly,

Table 1 Simple angular strain joint: comparison between skewed torque results (components of Euler vector in radians)

	"ground"		"node"		"invariant"
	analytical, MBDyn, Abaqus	MSC/ADAMS	analytical, MBDyn Abaqus	MSC/ADAMS	analytical, MBDyn
θ_x	0.	0.00000500	0.00082223	0.00082268	0.00043958
θ_y	0.00099998 ($\sin\alpha/k_2''$)	0.00099997	0.00091817	0.00091403	0.00097812
θ_z	0.00999950 ($\cos\alpha/k_3''$)	0.00999950	0.00999958	0.00999920	0.00999952

no invariant analytical solution could be found for a joint whose constitutive properties are referred to the halfway orientation between the nodes when a unit moment about global axis 3 is applied. Therefore, the numerical solution of (40) with the moment of (42) is reported as reference.

The attached angular spring element considered in this application is implemented in MBDyn, with the limitation described in footnote 2, by adding, on top of a spherical joint (a `spherical hinge` joint element of MBDyn's library), a standard (i.e., attached) `deformable hinge` joint element with a `linear elastic generic` (i.e., linear and anisotropic) constitutive law using the matrix of (41). Results obtained for the three different cases are coincident with those of the "analytical" columns of Table 1. The analysis confirms that the very same result is obtained after inverting the order of the connected nodes in the multibody model definition. Note that the invariant solution lies somehow in between the two attached cases.

The `JOINTC` element yields a rotation essentially coincident with the analytical and numerical solutions obtained by the proposed formulation in the invariant case. This result is expected, in view of the discussion presented in Appendix A, since the magnitude of the resulting angle, $\theta = 0.01005686$ radian, is limited.

The attached angular spring element can be obtained in MSC/ADAMS by adding a `FIELD` element on top of a spherical hinge joint. The documentation warns the reader that the element assumes small relative rotations, and the software sometimes warns the user when this assumption is violated. This clearly indicates that the `FIELD` element is not intended to withstand large relative rotations. There is no mention of the non-invariance of this element with respect to connectivity. No invariant formulation is available to the authors' knowledge. MSC/ADAMS results show a very good agreement[5] in the "ground" and "node" attached cases. This allows to infer that MSC/ADAMS' `FIELD` element implements angular springs in the attached form.

4.1.2 Angular strain behavior of homogeneous isotropic parallelepiped

A solid 3D model of a simple parallelepiped, shown in Fig. 2, is considered. The points indicated with A and B in the figure represent the locations of the nodes of the corresponding multibody model, a and b in the formulas. The side centered by each point is constrained to move rigidly.

[5]The difference on the last digits with respect to the reference results is possibly related to the fact that the relative orientation vector was computed from the Euler's parameters output by MSC/ADAMS with 6-digit accuracy.

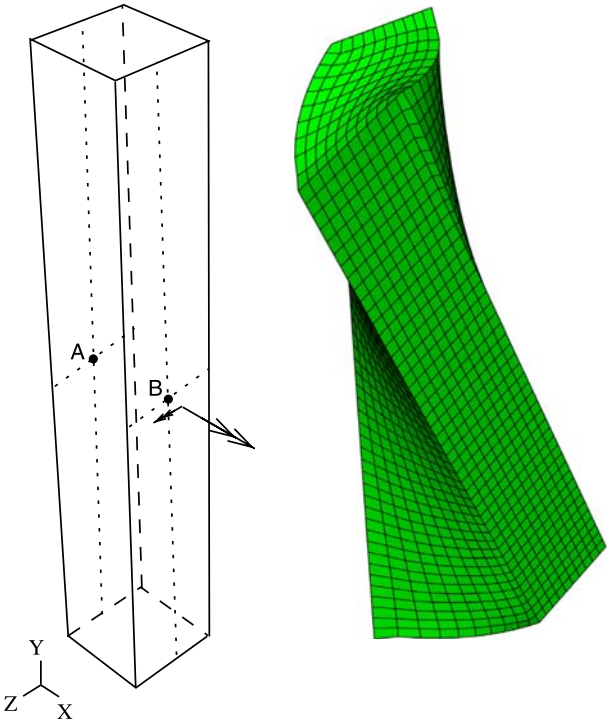

Fig. 2 Parallelepiped: sketch of the problem

Table 2 Properties of the parallelepiped model

Property		Value	Units
Base width (axis 1)	a	5.0	m
Height (axis 2)	b	30.0	m
Base length (axis 3)	c	5.0	m
Young's Modulus	E	1.0	N/m^2
Poisson's Modulus	ν	0.3	
Principal linear compliance 1	$1/k'_1$	2.92620×10^{-2}	m/N
Principal linear compliance 2	$1/k'_2$	9.14059×10^{-2}	m/N
Principal linear compliance 3	$1/k'_3$	1.26005×10^{-1}	m/N
Principal angular compliance 1	$1/k''_1$	1.59343×10^{-3}	radian/(Nm)
Principal angular compliance 2	$1/k''_2$	1.43837×10^{-2}	radian/(Nm)
Principal angular compliance 3	$1/k''_3$	4.00635×10^{-4}	radian/(Nm)

The geometrical and constitutive properties of the model are illustrated in Table 2. The parallelepiped is made of homogeneous isotropic material. The model has been analyzed with Abaqus/Standard, to obtain a static characterization in terms of linear and angular strain measures as functions of the applied force and moment. Table 2 also illustrates the resulting compliance properties. The simple manipulations required to obtain the decoupled linear and angular compliances shown in the table are detailed in Sect. 4.2. The orthotropy of

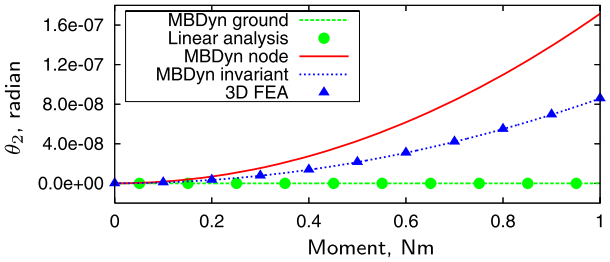

Fig. 3 Parallelepiped: component θ_2 of rotations obtained by different angular strain joint models and nonlinear 3D FEA for a moment not aligned with the principal axes (0 to 1 Nm). "Ground" and "node" refer to the attached case, respectively connected to the grounded and to the floating node

the structural component appears to be quite pronounced. This problem is not representative of any real artifact; it is only provided as a simple example of how the features of the proposed formulation can capture the details of the behavior of a nontrivial elastic deformable component.

Thanks to its symmetries, the principal axes can be easily identified as the axes orthogonal to the sides, intersecting the sides in their center. A side normal to axis 1 is grounded, and the opposite one is constrained to act as a rigid body, connected to a free node.

When a nonlinear 3D FE analysis of the same problem is performed, applying to the unconstrained side a moment about an axis nearly parallel to axis 1 (the one with the intermediate stiffness), but with a minimal component about axis 3 (the one with the largest stiffness), namely

$$\mathbf{m} = \left\{ \begin{array}{c} \cos\alpha \\ 0 \\ \sin\alpha \end{array} \right\}, \tag{43}$$

with $\tan\alpha = 0.01$, the rotation reported in Fig. 3 is obtained for component θ_2 of the rotation vector. As expected, the other components, θ_1 and θ_3 (not shown in the figure), which correspond to the non-null components of the moment $\mathbf{m}$, are indistinguishable from the linear case. The figure shows that the nonlinear analyses exhibit a nearly parabolic perturbation about axis 2, which is not directly loaded by the moment of (43), with the notable exception of the attached case when the constitutive properties are referred to the grounded node (indicated as "MBDyn ground").

When the invariant connectivity is used along with the linear constitutive properties of Table 2, the 3D FEA results are coincident with the curves obtained by the proposed angular joint implementation. Note that a purely linear analysis, also shown in Fig. 3, would have entirely missed the rotation about axis 2, which is small compared to those about axes 1 and 3 (between 1 and 4 orders of magnitude within the load range showed in the figure). Also, note that in case the attached formulation is used, but the constitutive properties are related to the orientation of the floating node (indicated as "MBDyn node" in the figures), the rotation component θ_2 would be approximately twice that resulting from the 3D FEA.

It is also worth mentioning that the results obtained with Abaqus/Standard's `JOINTC` element, not shown in Fig. 3, are coincident with those obtained with the 3D FEA and with the proposed invariant formula. The formulation of the `JOINTC` element is presented in Appendix A.

In conclusion, when linear elastic constitutive properties and linear elastic materials are considered, and the system is subjected to limited strains, the complexity of the problem is essentially dominated by the geometrical nonlinearity related to the finiteness of rotations. In this case, the proposed invariant formulation is consistent with nonlinear 3D FEA. On the contrary, the attached formulation, commonly used in lumped deformable component

models, could lead to either underestimating or overestimating the couplings introduced by the finiteness of rotations, depending on which node the constitutive properties are referred to.

When strains are no longer limited, the behavior of the proposed formulation departs from that of the nonlinear 3D FEA. To be able to yield more accurate results, the constitutive properties of the lumped component need to account for the nonlinear behavior of the actual component. This aspect is beyond the scope of the present work, and will be the subject of future activity.

Buckling may arise when a moment about a direction of larger stiffness can be resisted by the joint by twisting about a direction orthogonal to that moment, so that a lower energy state can be reached by the system by actually bending about a direction with smaller stiffness.

The perturbation of the moment of (37) yields

$$\delta\mathbf{m} = \mathbf{R}\big(\tilde{\boldsymbol{\theta}}(\xi)\big)\big(\mathbb{K} - \xi(\mathbb{K}\boldsymbol{\theta}) \times \boldsymbol{\Gamma}\big(\tilde{\boldsymbol{\theta}}(\xi)\big)^T\big)\delta\boldsymbol{\theta}, \tag{44}$$

where the property

$$\mathbf{R}(\boldsymbol{\theta})^T\boldsymbol{\Gamma}(\boldsymbol{\theta}) = \boldsymbol{\Gamma}(\boldsymbol{\theta})^T \tag{45}$$

of matrix $\boldsymbol{\Gamma}$ has been exploited (see [26]). The occurrence of buckling is indicated by

$$\det\big(\mathbb{K} - \xi(\mathbb{K}\boldsymbol{\theta}) \times \boldsymbol{\Gamma}\big(\tilde{\boldsymbol{\theta}}(\xi)\big)^T\big) = 0. \tag{46}$$

In configuration "ground," there is no possibility of buckling. On the contrary, configurations "node" and "invariant" are potentially prone to buckling. The analytical solution for the buckling of an orthotropic angular spring has been obtained by means of a symbolic manipulator when the moment is applied about a principal axis. The limit moment values in the node and invariant cases of this problem are 830.4555 and 415.2378 Nm, respectively.

Figure 4 illustrates the components of the rotation of the floating node when a static analysis is performed with MBDyn. The perturbation in the orientation of the moment, (43), triggers the instability while avoiding the singularity in the stiffness matrix. The rotation about axis 1 remains almost linear until buckling occurs; from that point on it almost settles. The rotation about axis 3 quickly departs from linearity, initially diverging while approaching buckling, and eventually settling to a nearly linear shape with much larger slope. The rotation about axis 2, which started as nearly parabolic according to Fig. 3, after the buckling eventually settles to a nearly constant value. It is worth noticing that the rotation about axis 2 obtained by the invariant connectivity at some point overcomes that obtained by the connectivity model that refers the constitutive properties to the floating node, and almost doubles it. No buckling occurs when the constitutive properties are attached to the ground. The numerical experiment confirms that for the invariant case the buckling occurs at twice the moment required by the attached case.

The different formulations show a radically different qualitative and quantitative behavior. As a consequence, the choice of the most appropriate connectivity model could be of paramount importance for the correct simulation of dynamical systems.

4.1.3 Angular strain behavior of homogeneous isotropic frustum

In order to assess the suitability of the proposed formulation in case the layout of the actual component is not symmetric with respect to the two nodes it connects, the (pyramidal) frustum illustrated in Fig. 5 has been modeled. Its properties are summarized in Table 3.

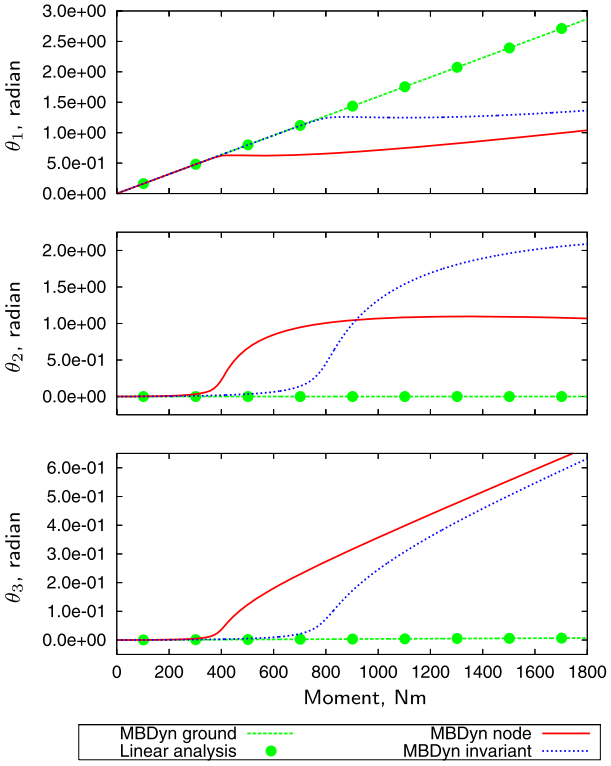

Fig. 4 Parallelepiped: rotations obtained by different angular strain joint models for a large moment not aligned with the principal axes (0 to 1800 Nm). "Ground" and "node" refer to the attached case, respectively connected to the grounded and to the floating node

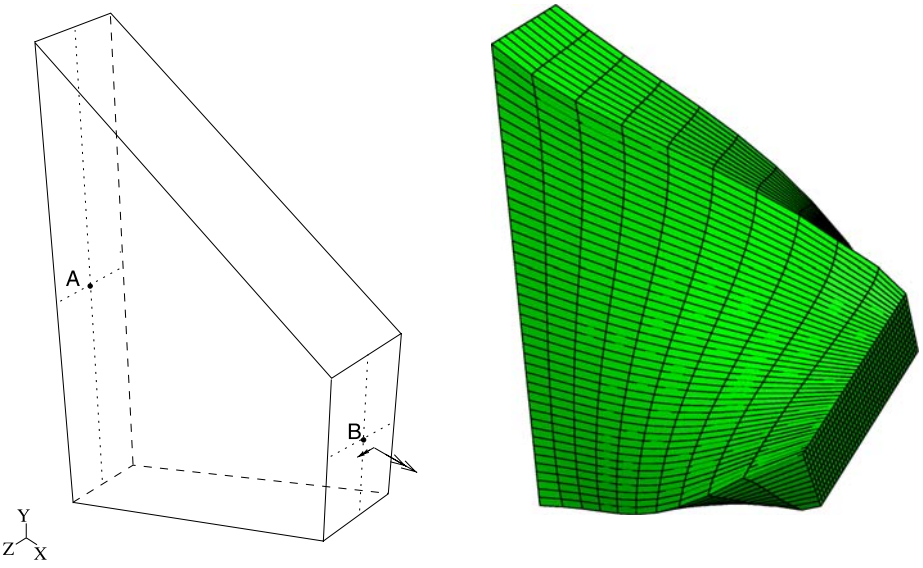

Fig. 5 Frustum: sketch of the problem

Table 3 Properties of the frustum model

Property		Value	Units
Height (axis 1)	a	10.0	m
Base length (axis 2)	b	30.0	m
Base width (axis 3)	c	5.0	m
Top length (axis 2)	b'	10.0	m
Top width (axis 3)	c'	5.0	m
Young's Modulus	E	1.0	N/m^2
Poisson's Modulus	ν	0.3	
Principal angular compliance 1	$1/k_1''$	6.39502×10^{-2}	radian/(Nm)
Principal angular compliance 2	$1/k_2''$	1.08390×10^{-1}	radian/(Nm)
Principal angular compliance 3	$1/k_3''$	1.28715×10^{-2}	radian/(Nm)

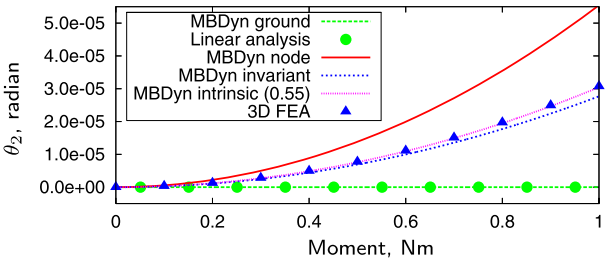

Fig. 6 Frustum: component θ_2 of rotations obtained by different angular strain joint models and by nonlinear 3D FEA for a moment not aligned with the principal axes (0 to 1 Nm). "Ground" and "node" refer to the attached case, respectively connected to the grounded and to the floating node

Figure 6 shows the result of the nonlinear 3D FEA compared to the results obtained by the proposed formulation. Note that when the invariant form is considered, a slight difference appears with respect to the nonlinear 3D FEA. However, a much better correlation can be found by fine tuning the parameter ξ that determines what weighted orientation the linear elastic constitutive properties of the lumped deformable component are referred to. In this case, a value $\xi = 0.55$ (namely, biased toward the top of the frustum) yields the expected results.

4.2 Simple linear/angular strain joint

Consider the 6D (linear and angular strain) compliance matrix $\mathbb{F}$ of a generic joint, obtained by independently loading with unit forces and moments one end, while keeping the other clamped, namely

$$\mathbb{F} = \begin{bmatrix} \mathbb{F}_{\mathbf{uf}} & \mathbb{F}_{\mathbf{um}} \\ \mathbb{F}_{\boldsymbol{\psi}\mathbf{f}} & \mathbb{F}_{\boldsymbol{\psi}\mathbf{m}} \end{bmatrix}. \tag{47}$$

The antidiagonal blocks $\mathbb{F}_{\mathbf{um}}$, $\mathbb{F}_{\boldsymbol{\psi}\mathbf{f}} (= \mathbb{F}_{\mathbf{um}}^T)$ couple moment to linear strain and force to angular strain. An attempt to decouple the linear from the angular behavior requires a linear transformation that redefines the moments in terms of the applied forces, namely

$$\begin{Bmatrix} \mathbf{f} \\ \mathbf{m} \end{Bmatrix} = \begin{bmatrix} \mathbf{I} & \mathbf{0} \\ \mathbf{A} & \mathbf{I} \end{bmatrix} \begin{Bmatrix} \mathbf{f}^* \\ \mathbf{m}^* \end{Bmatrix}, \tag{48}$$

which, according to the virtual complementary work principle, implies that

$$\left\{ \begin{array}{c} \mathbf{u}^* \\ \boldsymbol{\psi}^* \end{array} \right\} = \left[\begin{array}{cc} \mathbf{I} & \mathbf{A}^T \\ \mathbf{0} & \mathbf{I} \end{array} \right] \left\{ \begin{array}{c} \mathbf{u} \\ \boldsymbol{\psi} \end{array} \right\}. \tag{49}$$

According to (48) and (49), the compliance matrix becomes

$$\mathbb{F}^* = \left[\begin{array}{cc} \mathbf{I} & \mathbf{A}^T \\ \mathbf{0} & \mathbf{I} \end{array} \right] \left[\begin{array}{cc} \mathbb{F}_{\mathbf{uf}} & \mathbb{F}_{\mathbf{um}} \\ \mathbb{F}_{\mathbf{um}}^T & \mathbb{F}_{\boldsymbol{\psi}\mathbf{m}} \end{array} \right] \left[\begin{array}{cc} \mathbf{I} & \mathbf{0} \\ \mathbf{A} & \mathbf{I} \end{array} \right]. \tag{50}$$

The transformation matrix $\mathbf{A}$ is computed by setting to zero either of the antidiagonal blocks of the transformed compliance matrix, namely $\mathbf{A} = -\mathbb{F}_{\boldsymbol{\psi}\mathbf{m}}^{-1}\mathbb{F}_{\mathbf{um}}^T$. Only in case $\mathbf{A}$ is skew-symmetric, and thus $\mathbf{A} = \mathbf{x}\times$, the transformation corresponds to moving the joint location by $\mathbf{x}$ from the free node, in order to decouple forces and moments. The resulting compliance matrix is block-diagonal.

This procedure is not required since the implementation allows fully coupled 6D deformable components; however, it might be desirable in order to highlight the subtleties of the joint's behavior.

4.2.1 Linear/angular strain behavior of homogeneous isotropic parallelepiped

Consider again the parallelepiped of Fig. 2; the 6D compliance matrix, obtained by independently loading with unit forces and moments the free side normal to axis 1 of the finite element model, is

$$\mathbb{F} = \left[\begin{array}{cccccc} 2.926\text{e}{-2} & 0.000\text{e}{+0} & 0.000\text{e}{+0} & 0.000\text{e}{+0} & 0.000\text{e}{+0} & 0.000\text{e}{+0} \\ 0.000\text{e}{+0} & 9.391\text{e}{-2} & 0.000\text{e}{+0} & 0.000\text{e}{+0} & 0.000\text{e}{+0} & 1.002\text{e}{-3} \\ 0.000\text{e}{+0} & 0.000\text{e}{+0} & 0.216\text{e}{+0} & 0.000\text{e}{+0} & -3.596\text{e}{-2} & 0.000\text{e}{+0} \\ 0.000\text{e}{+0} & 0.000\text{e}{+0} & 0.000\text{e}{+0} & 1.593\text{e}{-3} & 0.000\text{e}{+0} & 0.000\text{e}{+0} \\ 0.000\text{e}{+0} & 0.000\text{e}{+0} & -3.596\text{e}{-2} & 0.000\text{e}{+0} & 1.438\text{e}{-2} & 0.000\text{e}{+0} \\ 0.000\text{e}{+0} & 1.002\text{e}{-3} & 0.000\text{e}{+0} & 0.000\text{e}{+0} & 0.000\text{e}{+0} & 4.006\text{e}{-4} \end{array} \right]. \tag{51}$$

The transformation matrix $\mathbf{A}$ is skew-symmetric (it is not, for example, in the case of the frustum); the position that decouples forces and moments appears to be $\mathbf{x} = \{-2.5, 0.0, 0.0\}$ m with respect to the point on the free side the compliance matrix was initially referred to, corresponding to the centroid of the parallelepiped, as one would expect. The corresponding principal compliance values have already been presented in Table 2.

The subsequent analysis shows the behavior of the parallelepiped when loaded at this special point. When a combination of compression in direction 1 and shear in direction 3, of equal magnitude, are applied to the problem, the system strains in the direction of the load, and the behavior is essentially linear, since the forces yield relatively small strains. Also, due to the orthotropy of the problem, the parallelepiped appears to bend about axis 2, as shown in Fig. 7, where the abscissa contains the magnitude of the force. This bending, however, is absent when the constitutive properties are attached to the ground, or excessive when the constitutive properties are attached to the floating node. Only the proposed formulation seems to capture the correct amount of bending. Note that even Abaqus/Standard's `JOINTC` element (not shown in the figure) either misses or overestimates the behavior of the component, resulting in the same behavior of the attached formulation, as opposed to the case of pure moment discussed in Sect. 4.1.2.

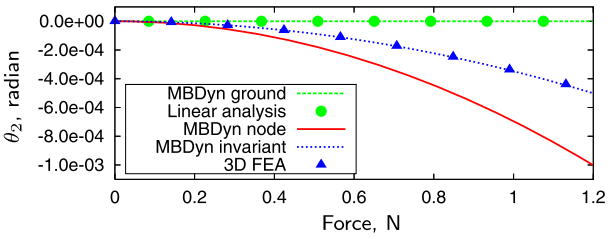

Fig. 7 Parallelepiped: component θ_2 of rotations when loaded by a force that is compressing in direction 1 (u_1), and shearing in direction 3 (u_3)

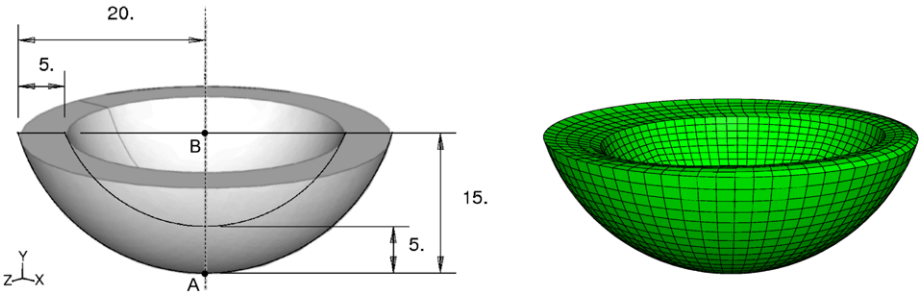

Fig. 8 Elastomeric bearing: sketch of the problem

4.2.2 Elastomeric bearing

This application addresses the model of an elastomeric bearing, illustrated in Fig. 8. It consists in two rigid spherical bowls, whose interstice is filled with isotropic material. A typical, critical application of this bearing occurs in the helicopter industry to connect helicopter rotor blades to the hub.

In terms of configuration- and history-dependent constitutive laws, this example does not address the requirements to model the behavior of real elastomeric bearings, which is far from linear elastic. However, the validity of what follows is not diminished by this consideration, given the clear separation between connectivity and constitutive properties pursued by the proposed formulation.

Because of its design, the linearized characterization of the component presents orthotropic constitutive properties. As a consequence, an incorrect modeling of the connectivity of the lumped deformable component would suffer from the problems highlighted in this work. To the authors' knowledge, none of the rotorcraft aeromechanics nor of the general-purpose multibody software typically used for this type of analysis, except MBDyn since version 1.3 [25], can model this type of lumped deformable components with the intrinsic connectivity properties proposed in this work.

The compliance matrix obtained from the 3D FEA, decoupled as illustrated in Sect. 4.2, yields the compliance properties of Table 4. The reference point lies along the joint's symmetry axis, slightly below the cut plane (14.7488 m from the plane tangent to the outer spherical bowl at the intersection with the symmetry axis). The constitutive properties of the structural component are isotropic in the plane normal to axis 2, and the orthotropy is not quite pronounced. Nonetheless, the component's behavior differs significantly from that of the parallelepiped considered in Sect. 4.2.1, due to its intrinsic lack of planar symmetry normal to the axis that connects the two nodes.

Figure 9 illustrates the unexpected bending behavior of the elastomeric bearing when subjected to simultaneous compression and shear: the nonlinear bending about axis 3 cou-

Table 4 Properties of the elastomeric bearing model

Property		Value	Units
Young's Modulus	E	1.0×10^5	N/m^2
Poisson's Modulus	ν	0.4	
Principal linear compliance 1	$1/k'_1$	4.9357×10^{-8}	m/N
Principal linear compliance 2	$1/k'_2$	3.4801×10^{-8}	m/N
Principal linear compliance 3	$1/k'_3$	4.9357×10^{-8}	m/N
Principal angular compliance 1	$1/k''_1$	6.3072×10^{-10}	radian/(Nm)
Principal angular compliance 2	$1/k''_2$	5.7187×10^{-10}	radian/(Nm)
Principal angular compliance 3	$1/k''_3$	6.3072×10^{-10}	radian/(Nm)

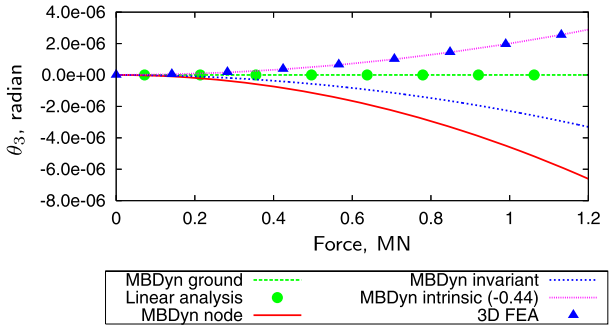

Fig. 9 Elastomeric bearing: component θ_3 of rotations obtained by different linear/angular strain joint models and by nonlinear 3D FEA for shear in principal direction 1 and compression in principal direction 2

pled to the applied forces is completely missed by all formulations, either attached or invariant. However, the intrinsic formulation allows to capture the behavior predicted by the nonlinear 3D FEA by selecting a rather unusual $\xi = -0.435917$, which means that the orientation in which the constitutive properties are evaluated must be significantly biased toward the first node, on the opposite side with respect to the second node. Moreover, the virtual point where the constitutive forces are applied when the component is strained, with the caveat of (34), moves beyond the second node, along the direction of the relative distance **d**, by an amount that is almost half the length of **d** itself.

The presented behavior has been assessed by analyzing different orientations of the applied force, resulting in different ratios between the compression and the shear force components. The value of ξ that allows the proposed formulation to match the results predicted by the 3D FEA is insensitive to the orientation of the force, thus appearing as an invariant property of the structural component. The bending rotation associated to the simultaneous presence of compression/tension and shear loads is proportional to the product of the two components of the loading force. In fact, a bending moment about axis 3 results from the product of the shear force along axis 1 by the arm represented by the displacement along axis 2 caused by the compression/tension force, which is essentially linear. This causes the observed parabolic behavior of the bending rotation component θ_3 with respect to the magnitude of the force, which vanishes in the case of pure compression/tension or shear.

The proposed results, although interesting, clearly show that the magnitude of the rotation induced by this second-order coupling in most cases can be considered negligible. This, however, is related to the choice of the geometrical and mechanical properties of the component.

5 Concluding remarks

This work illustrates how the formulation of lumped deformable components may depend on the reference the constitutive properties are expressed in when finite rotations need to be accounted for, as in nonlinear multibody dynamics.

A formulation of generic lumped linear and angular strain deformable components, that intrinsically does not depend on the order in which the element's connectivity is expressed, is presented. The proposed formulation has been implemented in the free general-purpose multibody analysis software MBDyn.

Its application to the modeling of arbitrarily anisotropic structural components is illustrated. A consistent approach for the computation of the constitutive properties of lumped deformable components from nonlinear finite element analysis is proposed and illustrated by means of examples of increasing complexity.

The outcome of the present work can be summarized in the following points:

1. It is important to have reliable lumped components that mimic the behavior of complex, detailed 3D systems for use in multibody analysis.
2. Nonlinearities related to geometrical aspects (finite rotations) may be separated from constitutive ones, when possible; this is the case when strains are small, which does not imply that the relative displacement and rotation between the connected nodes are small as well.
3. When strains are no longer small, nonlinearities in the constitutive law, related to strain finiteness, need to be accounted for; this is outside the scope of the present work, and will be addressed in future research.
4. The proposed invariant formula, with $\xi = 1/2$ in (10), allows to naturally deal with the geometrical nonlinearity of deformable components with symmetric layout.
5. The possibility to use an arbitrary value for ξ allows to tune the behavior of the lumped component to match the experimental behavior of non-symmetric layouts of the deformable components, by referring the constitutive properties to a suitably chosen weighted orientation.
6. At the very least, the proposed invariant formula prevents trivial modeling errors, like swapping the nodes that are connected by the lumped deformable component.

The main advantages of the proposed formulation over existing ones are:

(a) It naturally handles second-order couplings related to the geometry of finite rotations in anisotropic angular components (like Abaqus/Standard's `JOINTC`, but without the limitation to small rotations).
(b) It naturally handles second-order couplings related to the geometry of finite displacements and rotations in linear/angular components (unlike any other implementation known to the authors).
(c) It allows to mimic the behavior of components with arbitrary shape, provided the appropriate value of ξ can be determined (this feature is considered unique by the authors).
(d) It is based on an intrinsic definition of the linear and angular strains, and thus consistent nonlinear constitutive laws can be built upon its connectivity for arbitrarily large strain values.

To the authors' knowledge, there exists no other implementation of lumped deformable components that uses the relative rotation as the definition of the angular strain. This choice allows to separate geometrical from constitutive aspects in the modeling of components that are subjected to large relative displacements and rotations. This separation is expected to

ease the identification of appropriate constitutive laws of arbitrary complexity, and thus to improve the overall fidelity of multibody analysis.

Acknowledgements This work has been partially supported by Hutchinson Corporate Research Center. The authors gratefully acknowledge Mr. Benoualid's support to free software.

Appendix A: Abaqus/standard's `JOINTC` element

The components of the simplified angular strain $\overline{\boldsymbol{\psi}}$ used by Abaqus/Standard's `JOINTC` connection element [13] are

$$\psi_k = \frac{1}{2}(\mathbf{e}_{ib} - \mathbf{e}_{ia}) \cdot (\mathbf{e}_{jb} + \mathbf{e}_{ja}) \tag{52}$$

with $i = 1, 2, 3,\ j = 2, 3, 1,\ k = 3, 1, 2$. This corresponds to

$$\overline{\boldsymbol{\psi}} = \mathrm{ax}(\mathbf{R}_{\mathrm{rel}}) \tag{53a}$$

$$= \frac{\sin\theta}{\theta}\boldsymbol{\theta}, \tag{53b}$$

where $\theta = \|\boldsymbol{\theta}\|$, the so-called *linear parametrization* (see, for example [17]). Clearly, this expression can be considered a valid approximation of the relative rotation vector $\boldsymbol{\theta}$ only for small values of θ (strictly speaking, the relationship is invertible only for $\|\theta\| < \pi/2$).

The virtual work related to the rotation allowed by this element consists in

$$\delta\mathcal{L} = \delta\overline{\boldsymbol{\psi}} \cdot \overline{\mathbf{m}}, \tag{54}$$

where

$$\begin{aligned}\delta\psi_k = &\frac{1}{2}\big((\mathbf{e}_{jb} + \mathbf{e}_{ja}) \times \mathbf{e}_{ia} - (\mathbf{e}_{ib} - \mathbf{e}_{ia}) \times \mathbf{e}_{ja}\big)\boldsymbol{\theta}_{a\delta} \\ &- \frac{1}{2}\big((\mathbf{e}_{jb} + \mathbf{e}_{ja}) \times \mathbf{e}_{ib} + (\mathbf{e}_{ib} - \mathbf{e}_{ia}) \times \mathbf{e}_{jb}\big)\boldsymbol{\theta}_{b\delta}\end{aligned} \tag{55}$$

is the perturbation of the kth element of vector $\overline{\boldsymbol{\psi}}$, the simplified angular strain in node a's local reference frame. As such, the moments applied by the component to the nodes it connects are

$$\mathbf{m}_i = \frac{\partial}{\partial\boldsymbol{\theta}_{i\delta}}\delta\mathcal{L} = \left(\frac{\partial\overline{\boldsymbol{\psi}}}{\partial\boldsymbol{\theta}_{i\delta}}\right)^T \overline{\mathbf{m}}, \tag{56}$$

$i = a, b$. The gradient of the angular strain $\overline{\boldsymbol{\psi}}$ with respect to the nodes' angular degrees of freedom that left-multiplies the moment $\overline{\mathbf{m}}$ in (56) introduces the coupling that makes this formulation behave in a manner similar to the 3D analysis in Fig. 3. In fact, it plays the role of matrix $\hat{\mathbf{R}}$ in (19). The symmetry of (53a) shows that this formulation is not biased towards any of the nodes connected by the deformable component, so it has invariance properties similar to those of the proposed formula when $\xi = 1/2$. As a consequence, a constitutive law experimentally or numerically derived as a function of the relative rotation vector $\boldsymbol{\theta}$ could be transformed for $\overline{\boldsymbol{\psi}}$ for relatively small values of θ.

It is worth noticing that with respect to the linear strain, the `JOINTC` element does not exhibit the invariance properties of the proposed formulation with respect to node connectivity.

Appendix B: Proof of (28)

Consider (12); its perturbation yields

$$\begin{aligned}\delta\mathbf{R}_{\text{rel}}\mathbf{R}_{\text{rel}}^T &= \boldsymbol{\theta}_\delta \times \\ &= \delta\tilde{\mathbf{R}}\big(\tilde{\boldsymbol{\theta}}(\xi)\big)\tilde{\mathbf{R}}\big(\tilde{\boldsymbol{\theta}}(\xi)\big)^T \\ &\quad + \tilde{\mathbf{R}}\big(\tilde{\boldsymbol{\theta}}(\xi)\big)\delta\tilde{\mathbf{R}}\big(\tilde{\boldsymbol{\theta}}(1-\xi)\big)\tilde{\mathbf{R}}\big(\tilde{\boldsymbol{\theta}}(1-\xi)\big)^T\tilde{\mathbf{R}}\big(\tilde{\boldsymbol{\theta}}(\xi)\big)^T \\ &= \tilde{\boldsymbol{\theta}}_\delta(\xi) \times + \tilde{\mathbf{R}}\big(\tilde{\boldsymbol{\theta}}(\xi)\big)\tilde{\boldsymbol{\theta}}_\delta(1-\xi) \times \tilde{\mathbf{R}}\big(\tilde{\boldsymbol{\theta}}(\xi)\big)^T, \end{aligned} \tag{57}$$

or

$$\begin{aligned}\boldsymbol{\theta}_\delta &= \tilde{\boldsymbol{\theta}}_\delta(\xi) + \tilde{\mathbf{R}}\big(\tilde{\boldsymbol{\theta}}(\xi)\big)\tilde{\boldsymbol{\theta}}_\delta(1-\xi) \\ &= \xi\boldsymbol{\Gamma}(\xi\boldsymbol{\theta})\boldsymbol{\Gamma}(\boldsymbol{\theta})^{-1}\boldsymbol{\theta}_\delta + (1-\xi)\tilde{\mathbf{R}}\big(\tilde{\boldsymbol{\theta}}(\xi)\big)\boldsymbol{\Gamma}\big((1-\xi)\boldsymbol{\theta}\big)\boldsymbol{\Gamma}(\boldsymbol{\theta})^{-1}\boldsymbol{\theta}_\delta \end{aligned} \tag{58}$$

Define

$$\tilde{\mathbf{I}}(\xi) = \xi\boldsymbol{\Gamma}(\xi\boldsymbol{\theta})\boldsymbol{\Gamma}(\boldsymbol{\theta})^{-1}; \tag{59}$$

(58), which is valid for an arbitrary value of $\boldsymbol{\theta}_\delta$, implies

$$\mathbf{I} = \tilde{\mathbf{I}}(\xi) + (1-\xi)\tilde{\mathbf{R}}\big(\tilde{\boldsymbol{\theta}}(\xi)\big)\boldsymbol{\Gamma}\big((1-\xi)\boldsymbol{\theta}\big)\boldsymbol{\Gamma}(\boldsymbol{\theta})^{-1}. \tag{60}$$

Now, from (12),

$$\tilde{\mathbf{R}}\big(\tilde{\boldsymbol{\theta}}(\xi)\big) = \mathbf{R}_{\text{rel}}\tilde{\mathbf{R}}\big(\tilde{\boldsymbol{\theta}}(1-\xi)\big)^T, \tag{61}$$

and, according to (45),

$$\mathbf{R}_{\text{rel}} = \boldsymbol{\Gamma}(\boldsymbol{\theta})^{-T}\boldsymbol{\Gamma}(\boldsymbol{\theta}), \tag{62}$$

while

$$\tilde{\mathbf{R}}\big(\tilde{\boldsymbol{\theta}}(1-\xi)\big)^T\boldsymbol{\Gamma}\big((1-\xi)\boldsymbol{\theta}\big) = \boldsymbol{\Gamma}\big((1-\xi)\boldsymbol{\theta}\big)^T. \tag{63}$$

Equation (60) becomes

$$\begin{aligned}\mathbf{I} &= \tilde{\mathbf{I}}(\xi) + (1-\xi)\boldsymbol{\Gamma}(\boldsymbol{\theta})^{-T}\boldsymbol{\Gamma}(\boldsymbol{\theta})\boldsymbol{\Gamma}\big((1-\xi)\boldsymbol{\theta}\big)^T\boldsymbol{\Gamma}(\boldsymbol{\theta})^{-1} \\ &= \tilde{\mathbf{I}}(\xi) + (1-\xi)\boldsymbol{\Gamma}(\boldsymbol{\theta})^{-T}\boldsymbol{\Gamma}\big((1-\xi)\boldsymbol{\theta}\big)^T\boldsymbol{\Gamma}(\boldsymbol{\theta})\boldsymbol{\Gamma}(\boldsymbol{\theta})^{-1} \\ &= \tilde{\mathbf{I}}(\xi) + \tilde{\mathbf{I}}(1-\xi)^T. \end{aligned} \tag{64}$$

Appendix C: Special properties of matrix $\tilde{\mathbf{R}}$

The proposed formulas, in their practical implementation, will eventually need to be perturbed in order to compute the components' contribution to the Jacobian matrix of the problem, if they are incorporated in an implicit solution procedure. A detailed description of the related operations is given in MBDyn's theory manual [27].

A perturbation of the relative orientation yields

$$\boldsymbol{\theta}_\delta \times = \delta\mathbf{R}_{\text{rel}}\mathbf{R}_{\text{rel}}^T$$

$$= \delta\tilde{\mathbf{R}}\tilde{\mathbf{R}}^T + \tilde{\mathbf{R}}\delta\tilde{\mathbf{R}}\tilde{\mathbf{R}}^T\tilde{\mathbf{R}}^T$$

$$= \tilde{\boldsymbol{\theta}}_\delta \times + \tilde{\mathbf{R}}\tilde{\boldsymbol{\theta}}_\delta \times \tilde{\mathbf{R}}^T; \tag{65}$$

as a consequence,

$$\tilde{\boldsymbol{\theta}}_\delta = (\mathbf{I} + \tilde{\mathbf{R}})^{-1}\boldsymbol{\theta}_\delta. \tag{66}$$

Note that matrix $(\mathbf{I} + \tilde{\mathbf{R}})$ is singular for $\|\tilde{\boldsymbol{\theta}}\| = \pi$ radian, which introduces a limitation on the amount of angular strain the linear and the linear/angular deformable components can withstand.

Matrix $(\mathbf{I} + \tilde{\mathbf{R}})$, whose inverse is at the core of the definition of matrix $\hat{\mathbf{I}}$ in (32), has the interesting property of being invariant with respect to a pair of rotations $\tilde{\mathbf{R}}$ and $\tilde{\mathbf{R}}^T$, regardless of their order. In fact, the following properties can be easily verified:

$$\tilde{\mathbf{R}}^T(\mathbf{I} + \tilde{\mathbf{R}}) = \left(\mathbf{I} + \tilde{\mathbf{R}}^T\right), \tag{67}$$

$$(\mathbf{I} + \tilde{\mathbf{R}})\tilde{\mathbf{R}}^T = \left(\mathbf{I} + \tilde{\mathbf{R}}^T\right). \tag{68}$$

Another important property is:

$$\mathbf{I} - (\mathbf{I} + \tilde{\mathbf{R}})^{-1} = \left(\mathbf{I} + \tilde{\mathbf{R}}^T\right)^{-1}. \tag{69}$$

These properties may be interpreted in view of the affinity of matrix $(\mathbf{I}+\tilde{\mathbf{R}})$ with Cayley's parametrization of rotations. In fact, the parametrization of rotations that exploits Cayley's transform, as described in [28], is based on the property

$$\tilde{\mathbf{R}} = (\mathbf{I} + \boldsymbol{\zeta} \times)(\mathbf{I} - \boldsymbol{\zeta} \times)^{-1} \tag{70a}$$

$$= (\mathbf{I} - \boldsymbol{\zeta} \times)^{-1}(\mathbf{I} + \boldsymbol{\zeta} \times), \tag{70b}$$

a special case of (45), which states that either of the products at the right-hand side of (70) yields an orthonormal matrix with positive unit determinant.

The relationship

$$(\mathbf{I} + \tilde{\mathbf{R}})^{-1} = \frac{1}{2}(\mathbf{I} - \boldsymbol{\zeta} \times) \tag{71}$$

can be obtained with some manipulation of either of (70), remembering that Cayley's parametrization consists in

$$\boldsymbol{\zeta} = \frac{1}{\tilde{\theta}} \tan\left(\frac{\tilde{\theta}}{2}\right)\tilde{\boldsymbol{\theta}}. \tag{72}$$

Equation (71) represents a computationally efficient manner to compute the inverse of matrix $(\mathbf{I} + \tilde{\mathbf{R}})$ avoiding a (trivial: 3×3) matrix inversion, at the cost of evaluating a trigonometric function.

References

1. Shabana, A.A.: Dynamics of Multibody Systems, 2nd edn. Cambridge University Press, Cambridge (1998)

2. Schiehlen, W.: Multibody system dynamics: Roots and perspectives. Multibody Syst. Dyn. **1**(2), 149–188 (1997). doi:10.1023/A:1009745432698
3. Shabana, A.A.: Flexible multibody dynamics: Review of past and recent developments. Multibody Syst. Dyn. **1**(2), 189–222 (1997). doi:10.1023/A:1009773505418
4. Wasfy, T.M., Noor, A.K.: Computational strategies for flexible multibody systems. Appl. Mech. Rev. **56**(6), 553–613 (2003). doi:10.1115/1.1590354
5. Pan, W., Haug, E.J.: Dynamic simulation of general flexible multibody systems. Mech. Based Des. Struct. Mach. **27**(2), 217–251 (1999). doi:10.1080/08905459908915697
6. Wallrapp, O., Schwertassek, R.: Representation of geometric stiffening in multibody system simulation. Int. J. Numer. Methods Eng. **32**, 1833–1850 (1991). doi:10.1002/nme.1620320818
7. Ambrósio, J.A.C.: Dynamics of structures undergoing gross motion and nonlinear deformations: A multibody approach. Comput. Struct. **59**(6), 1001–1012 (1996). doi:10.1016/0045-7949(95)00349-5
8. Géradin, M., Cardona, A.: Flexible Multibody Dynamics: a Finite Element Approach. Wiley, Chichester (2001)
9. Shabana, A.A., Schwertassek, R.: Equivalence of the floating frame of reference approach and finite element formulations. Int. J. Non-Linear Mech. **33**(3), 417–432 (1998). doi:10.1016/S0020-7462(97)00024-3
10. Ledesma, R., Ma, Z.-D., Hulbert, G., Wineman, A.: A nonlinear viscoelastic bushing element in multibody dynamics. Comput. Mech. **17**(5), 287–296 (1996). doi:10.1007/BF00368551
11. Kadlowec, J., Wineman, A., Hulbert, G.: Elastomer bushing response: experiments and finite element modeling. Acta Mech. **163**, 25–38 (2003). doi:10.1007/s00707-003-1018-1
12. MSC/ADAMS User's Manual, 2007
13. Abaqus Theory Manual, Abaqus Version 6.7 edition
14. Merel, J., Wander, I., Masarati, P., Morandini, M.: Analysis of load patterns in rubber components for vehicles. In: Multibody Dynamics 2007, ECCOMAS Thematic Conference, pp. 1–19, Milan, June 25–28, 2007
15. Pfister, F.: Bernoulli numbers and rotational kinematics. J. Appl. Mech. **65**(3), 758–763 (1998). doi:10.1115/1.2789120
16. Betsch, P., Menzel, A., Stein, E.: On the parametrization of finite rotations in computational mechanics. A classification of concepts with application to smooth shells. Comput. Methods Appl. Mech. Eng. **155**(3–4), 273–305 (1998). doi:10.1016/S0045-7825(97)00158-8
17. Bauchau, O.A., Trainelli, L.: The vectorial parameterization of rotation. Nonlinear Dyn. **32**(1), 71–92 (2003). doi:10.1023/A:1024265401576
18. Borri, M., Trainelli, L., Bottasso, C.L.: On representations and parameterizations of motion. Multibody Syst. Dyn. **4**(2–3), 129–193 (2000). doi:10.1023/A:1009830626597
19. Merlini, T., Morandini, M.: The helicoidal modeling in computational finite elasticity. part II: multiplicative interpolation. Int. J. Solids Struct. **41**(18–19), 5383–5409 (2004). doi:10.1016/j.ijsolstr.2004.02.026
20. Shoemake, K.: Animating rotation with quaternion curves. SIGGRAPH Comput. Graph. **19**(3), 245–254 (1985)
21. Borri, M., Bottasso, C.L.: An intrinsic beam model based on a helicoidal approximation—part I: Formulation. Intl. J. Numer. Methods Eng. **37**, 2267–2289 (1994). doi:10.1002/nme.1620371308
22. Jelenić, G., Crisfield, M.A.: Geometrically exact 3D beam theory: implementation of a strain-invariant finite element for statics and dynamics. Comput. Methods Appl. Mech. Eng. **171**, 141–171 (1999)
23. Krenk, S.: A vector format for conservative time integration of rotations. In: Multibody Dynamics 2007, ECCOMAS Thematic Conference, pp. 1–12, Milan, June 25–28, 2007
24. Cardona, A., Geradin, M.: A beam finite element non-linear theory with finite rotations. Int. J. Numer. Methods Eng. **26**, 2403–2438 (1988)
25. MBDyn Input Manual (Version 1.3) (2007)
26. Merlini, T.: Recursive representation of orthonormal tensors. DIA-SR 03-02, Dip. Ing. Aerospaziale, Politecnico di Milano (2003)
27. MBDyn Technical Manual (Version 1.3) (2007)
28. Trainelli, L.: On the parameterization of rotation and rigid motion: a comprehensive picture. In: 17th Congresso nazionale AIDAA, pp. 1349–1362, Rome, Italy, September 15–19, 2003